

# Anisotropic mechanism on distinct transition modes of tip-activated multipolarization switching in epitaxial BiFeO<sub>3</sub> films

Y. P. Shi,<sup>1</sup> A. K. Soh,<sup>1,a)</sup> and G. J. Weng<sup>2</sup>

<sup>1</sup>*Department of Mechanical Engineering, The University of Hong Kong, Hong Kong, China*

<sup>2</sup>*Department of Mechanical and Aerospace Engineering, Rutgers University, New Brunswick, New Jersey 08903, USA*

(Received 6 September 2010; accepted 26 November 2010; published online 19 January 2011)

Based on the extended Kittel's law, an anisotropic mechanism has been developed to investigate the complex multipolarization switching in (001) and (110) epitaxial BiFeO<sub>3</sub> films, under a biased-tip field. Switching inhomogeneity and domain wall width evolution have been specifically accounted for. It has been found that distinct switching modes, i.e., the breakdown mode of 71°-switched domain and the activation mode of 180°/109° switching, exist and dominate the switching orders within switching process. Our predicted switching orders show excellent agreements with the existing experimental data and phase-field results. A two-step procedure is also proposed to fabricate single-phase 71° ferroelastic domain array of controllable density using (001) BiFeO<sub>3</sub> films, which is favored in practice to significantly enhance the magnetoelectric coupling and photovoltage. © 2011 American Institute of Physics. [doi:10.1063/1.3532001]

## I. INTRODUCTION

Single-phase multiferroics (MFs) at room-temperature show intriguing applications for the realization of magnetoelectric (ME) coupling and high-density nonvolatile information storage. These technological applications rely on the distinct multifunctionalities of intrinsic domain walls (DWs) in reversibly switched domains. In addition to the essential function of buffering the polarization discontinuity and the stress gradient induced by antidirection of phases, DW has been reported to play prominent roles in enhancing strain-mediated ME coefficient by increasing elastic coupling,<sup>1</sup> creating above band gap photovoltage by separating photoexcited electron-hole pairs,<sup>2</sup> determining conduction properties of BiFeO<sub>3</sub> (Ref. 3) and YMnO<sub>3</sub> (Ref. 4) by lowering their band gaps, expediting polarization fatigue,<sup>5</sup> and in affecting the overall elastic modulus of bulk films.<sup>6</sup> Kinetically, thermodynamic stability of MF single-phase domains and macroscopic polarization switching mechanism can also be dramatically influenced by DW and its motion. This is because DWs and their intersections always act as strong sites for domain nucleation<sup>7</sup> and a dominant source for back-switching.<sup>8</sup> Besides, a slight broadening of DW width was found to significantly affect the measured coercive field.<sup>9</sup> However, there is a significant discrepancy between the experimental DW width data and the corresponding theoretical prediction of only several lattices in width.<sup>9</sup> This is most probably due to the negligence of the preponderant surface relaxation in theoretical predictions. We thus believe that a fundamental phenomenon involving the evolution of DW width may exist throughout the whole switching process to minimize the MF total energy. Although this phenomenon has never been systematically investigated, it could govern the complicated and seemingly “uncontrollable” switching process in rhombohedral BiFeO<sub>3</sub> (BFO) and hexagonal

YMnO<sub>3</sub> films. Hence, two essential questions would need to be answered to make controllable domain/DW-based devices: (i) how will MF DW width evolve subject to its deciding parameters change which includes, among others, the activating field, switching type, domain size, and level of inhomogeneity due to MF dielectric anisotropy as well as symmetry-breaking defects? (ii) How to realize a deterministic control of the practically favored ferroelastic switching or effectively suppressing the undesirable ferroelectric transition by utilizing possible distinct modes among optional ferroelastic/electric switching types?

## II. THEORY

To address these fundamental issues, a theoretical investigation is carried out in this work on the switching mechanism in both (001) and (110) epitaxial rhombohedral BFO thin films. We choose these systems because of their promising technological applications.<sup>10</sup> As shown in Figs. 1(a) and 1(b), the initial BFO matrix with a downward pseudocubic polarization vector  $\mathbf{P}_0$  ( $r1^-$  state) is switched by a biased-tip of piezoresponse force microscopy. This tip-activated switching fashion has been reported to hold the feasibility of stabilizing the otherwise unstable X9° domains by the tip-engineered DW architecture<sup>8</sup> and to effectively prevent the switched domains from elastic relaxation by fabricating isolated BFO monodomain islands.<sup>11</sup> To maintain consistency with well-studied cases, the applied tip-field is taken to be along the epitaxial direction of BFO film. Under the SPM-tip field with rotational in-plane symmetry and ultrahigh out-of-plane inhomogeneity, BFO thin films were discovered to experience film-orientation dependent switching phenomena. It was experimentally shown that the (001) epitaxial film written with an increased tip-bias was switched in the form of 71° ( $r3^+$ ) ferroelastic  $\rightarrow$  180° ( $r1^+$ ) ferroelectric switching,<sup>12,13</sup> whereas a transition order of

<sup>a)</sup>Electronic mail: aksoh@hkucc.hku.hk.

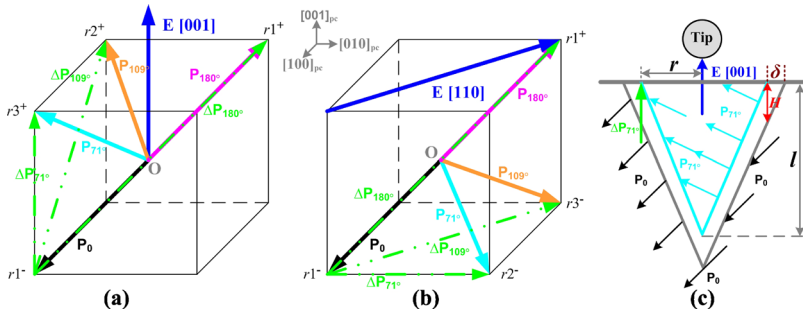


FIG. 1. (Color online) Schematics of multipolarization switching activated by a SPM-tip field in (a) (001) and (b) (110) BiFeO<sub>3</sub> thin films. Subscript  $\varphi$  denotes the angle of rotation from the initial  $\mathbf{P}_0$  to  $\mathbf{P}$ , and  $\Delta\mathbf{P}$  represents PDV pointing from  $\mathbf{P}_0$  to  $\mathbf{P}_\varphi$ . (c) Cross-sectional schematic of 71°-switched conic-domain-structure and polarization states formed in (001) BiFeO<sub>3</sub> film.

180°( $r1^+$ ) → 109°( $r3^-$ ) → 71°( $r2^-$ ) occurred in the (110) BFO film.<sup>8</sup> Regarding these widely distinct switching forms, we attribute them to different spatial configurations describing the relative orientation between each polarization difference vector (PDV),  $\Delta\mathbf{P}_\varphi$ , and the tip-field  $\mathbf{E}$  in the two epitaxial BFO films.  $\mathbf{P}_\varphi$  denotes the polarization vector switched from  $\mathbf{P}_0$  by an angle of  $\varphi=71^\circ$ ,  $109^\circ$ , or  $180^\circ$ , and  $P_s$  is the room-temperature spontaneous polarization of rhombohedral BFO, then  $\Delta\mathbf{P}_\varphi = \mathbf{P}_\varphi - \mathbf{P}_0$  with a magnitude of  $2P_s \sin(\varphi/2)$ . It should be noted that  $\mathbf{P}_\varphi$  is deemed only rotate from  $\mathbf{P}_0$  around cubic center with a fixed magnitude of  $P_s$ , due to the polarization compatibility<sup>14</sup> and some fluctuation of the stable polarization vector's equilibrium direction induced by the strong coupling effect between polar displacement and oxygen octahedral tilt, which does not affect polarization magnitude.<sup>15</sup> Consequently, each switched-component of  $\mathbf{P}_\varphi$  will be required to merely revert its direction and stabilize simultaneously polarization gradient within DW width along the direction of  $\Delta\mathbf{P}_\varphi$ . Drawing from the consistency between this requirement with characteristics of well-studied 180° ferroelectric DW, either the classical kink solution<sup>16</sup> or perturbative solution<sup>17</sup> can be introduced to describe the magnitude variation in PDV across DW

$$\overline{\Delta\mathbf{P}_\varphi}(S) = P_s \sin(\varphi/2) \tanh(2S/H), \quad (1)$$

where  $H$  is the *real* DW width parallel to PDV and  $S$  denotes the distance from DW center along the direction of PDV.

On the other hand, the extended Kittel's (EK's) law,<sup>18</sup> which extends the original Kittel law to include the effect of DW thickness and states the proportionality between the thickness of polarity film and the ratio of domain-periodicity square to DW width, will also be adopted to include the effect of DW width evolution. Although it covers both domain volume energy and DW energy and also shows validity to magneto/ferroelectric domains within or without isotropic fields,<sup>18</sup> it should be reminded that the original EK law will breakdown and need modification in our studied case. This results from both the inhomogeneous tip-field<sup>7</sup> and the mobile charges accumulation on flat DW surfaces<sup>5</sup> or sharp DW junctions,<sup>19</sup> which will directly favor certain polarization orientations and thus destabilize the "stable" EK's domain structures. Hence it is necessary to introduce an anisotropy exponent,  $n$ , to make an extension of EK's law, so that it can well represent the inhomogeneous polarization switching of BFO domains written by a biased SPM-tip. By replacing the film thickness and periodicity in the standard EK law with

formed domain length of  $l$  (growing along the  $\mathbf{E}$  direction) and in-plane radius of  $r$ ,<sup>19</sup> respectively [see Fig. 1(c)], the EK law can be modified (the details are given in the Appendix) as

$$r^n \eta = M \delta, \quad (2)$$

where  $M$  is a dimensionless constant, and  $\delta$  denotes the *measured* in-plane DW width. Domain aspect ratio  $\eta$  is defined as the ratio between radius  $r$  and a renormalized length  $L = l/\gamma$ , here the dielectric anisotropy  $\gamma = \sqrt{\epsilon_l/\epsilon_r}$  in terms of the longitudinal ( $\epsilon_l$ ) and radial ( $\epsilon_r$ ) dielectric constants of BFO. As will be shown below, this anisotropy exponent can decrease from its upper-bound to 1 under the effect of increased tip-voltage, and when  $n=1$ , Eq. (2) recovers the standard EK law.

Furthermore, it is necessary to make a distinction between the *measured* DW width  $\delta$  and the *real* DW thickness  $H$ . The difference between them lies in that current measurements of  $\delta$  are always implemented only in an ultrathin layer beneath the film surface. On the contrary,  $H$  can even display non-in-plane projection during switching when  $\varphi=71^\circ$  for the (001) BFO film or  $\varphi=109^\circ$  for the (110) case, which makes  $\delta$  measurements more difficult or even incredible. Detailed analysis of the geometrical constraint imposed by rhombohedral perovskite lattice<sup>20</sup> leads to an analytical connection between them as  $H=C\delta$ , where the geometry factor  $C = \gamma/\eta$ ,  $\sqrt{2}$ ,  $\sqrt{6}/2$  for 71°, 109°, and 180° switching, respectively, in the epitaxial (001) BFO film, whereas  $C = \sqrt{2}$ ,  $\gamma/\eta$ , and  $\sqrt{3}$  in the (110) film

Since the main driving force of multipolarization switching comes from the dynamical minimization of BFO domain total energy, any final stable single-phase state will also correspond to such a minimal energy state.<sup>12,19</sup> Benefiting from the recent analytical and effective inclusion of depolarization effect in our conic-domain-based mechanism,<sup>19</sup> we assume that the switched BFO domains will be conic in shape. Let  $\theta$  represent the separation angle between PDV and tip-field, the effective polarization difference switched by  $\mathbf{E}$  should be  $|\Delta\mathbf{P}_\varphi| = 2P_s \sin(\varphi/2) \cos \theta$ . In view that the stability of equilibrium domains in MF matrix unpractically extends to small size,<sup>8,11</sup> any stable BFO domain should not be smaller than a critical radius  $R$  of tens nanometer, which is in line with the typical size of narrow domains,<sup>4</sup> the smallest stable domain size,<sup>21</sup> or the "subcritical" nucleus.<sup>22</sup> Based on our previous theory,<sup>19</sup> the satisfaction of  $\varphi$ -switched domain larger than  $R_\varphi$  in radius leads to the minimal charge amount  $Q$  stored in the tip-sample capacitor

$$Q = \frac{\sqrt{\varepsilon_r \varepsilon_f} R_\varphi}{2f_\eta |\Delta P_\varphi|} \left[ \frac{3\eta R_\varphi |\Delta P_\varphi|^2}{8\varepsilon_r \cos^2 \theta} + \frac{\gamma \sigma_{\text{DW}}}{\eta} \right], \quad (3)$$

where  $f_\eta = 1 - \eta/2 + \eta \ln(2/\eta)$ , and  $\sigma_{\text{DW}}$  denotes the averaged energy density of DW. Since the dominant contribution of DW energy comes from polarization gradient,  $\sigma_{\text{DW}}$  is approximated from Eq. (1) as

$$\sigma_{\text{DW}} = \frac{g}{H} \int_{-\infty}^{\infty} \left( \frac{\partial \overline{\Delta P_\varphi}}{\partial S} \right)^2 dS = \frac{8gP_0^2 \sin^2(\varphi/2)}{3H^2}, \quad (4)$$

where  $g$  is the gradient energy coefficient. Although it seems that Eq. (4) excludes the ferroelastic component of DW energy, which may contribute significantly to the domain total energy,<sup>11</sup> it is worth pointing out that both parameters  $M$  in Eq. (2) and  $g$  in Eq. (4) have indirectly included the effect of ferroelastic energy and the magnetization energy, which arises directly from the intrinsic DW-mediated ME coupling between the tip-field activated polarization and its resultant magnetization, according to the recently proposed Dzyaloshinskii–Moriya interaction.<sup>23,24</sup> It is remarkable that in maintaining excellent consistency with the recent first-principle calculation results of Lubk *et al.*,<sup>25</sup> who reported that the stable DW energies for 71°, 109°, and 180° walls in the BFO supercell were 363 mJ/m<sup>2</sup>, 205 mJ/m<sup>2</sup>, and 829 mJ/m<sup>2</sup>, respectively, Eq. (4) predicts that the actual width of 109° DW is about two times that of the 71° DW in BFO film; in addition, the width of 180° BFO DW of ferroelectric type is indeed much narrower than that of the ferroelastic type, which is widely expected by researchers. By substituting Eqs. (2) and (4) to Eq. (3) and then minimizing  $Q$  with respect to  $R_\varphi$ , we obtain the critical domain radius (or DW width) and minimal charge as

$$\begin{cases} R_\varphi^{2n+1} = \frac{\zeta(2n-1)}{C^2 \eta^4}, \text{ or, } \delta_\varphi = \frac{\eta}{M} \left[ \frac{\zeta(2n-1)}{C^2 \eta^4} \right]^{n/2n+1} \\ Q_\varphi \geq \frac{3\gamma\eta \sin(\varphi/2) P_S R_\varphi^2}{4f_\eta \cos \theta_\varphi} \left( \frac{1}{2} + \frac{1}{2n-1} \right) \end{cases}, \quad (5)$$

where  $\zeta = 8g\gamma\varepsilon_r M^2/9$  can be considered as a characteristic variable to determine the BFO minimal stable radius. The condition of  $\zeta$  far less than 1 yields  $\partial Q_\varphi / \partial n < 0$ , which implies that commonly used poling fashion with a increasing tip-bias/charge will inevitably result in the occurrence of a polarization switching form manifesting an intrinsic decrease in its anisotropy exponent.

### III. DISCUSSION AND VALIDATION

This voltage-dependent switching mechanism can be adopted to analytically explain the ‘‘surprising’’ observations that low tip-voltage favored 71° ferroelastic switching whereas the 180° ferroelectric type proceeded under higher voltage in (001) BFO film.<sup>11,13</sup> It is shown from Eq. (5) that  $R_\varphi^{2n+1}$  is independent of switching angle, and when both  $\zeta$  and  $n$  are given, it is inversely proportional to  $\eta^2 \gamma^2$ ,  $2\eta^4$ , and  $1.5\eta^4$ , respectively, for 71°, 109°, and 180° switching in (001)-oriented BFO film as well as to  $2\eta^4$ ,  $\eta^2 \gamma^2$ , and  $3\eta^4$  in (110) film. In addition to the well-accepted statement that

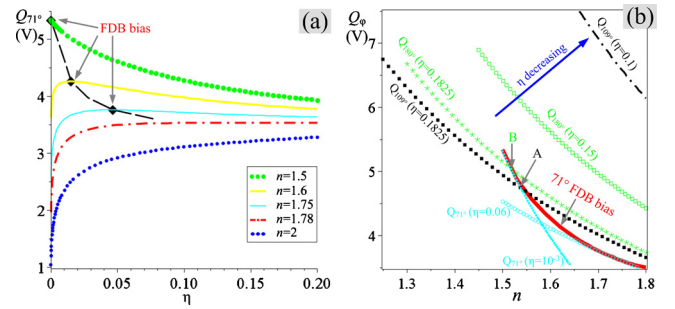


FIG. 2. (Color online) (a) Variation in  $Q_{71^\circ}$  vs  $\eta$  for various  $n$ . The dashed curve is a guide indicating the critical  $\eta$  variation in FDB. (b) Theoretical predictions of the competitive multipolarization switching in (001) epitaxial BFO film, poled by SPM-tip with an increasing voltage from 3.5 to 6.5 V. Point A and B represent the starting points for a stable nucleation of 109° and 180°-switched domain, respectively.

intrinsic depolarization field induces rapid elongation of switched domains,<sup>13</sup> we also found that the aspect ratio of a conic reverted domain in ferroelectrics should not exceed a threshold of  $\eta^{\text{max}} = 0.1825$ .<sup>19</sup> Building upon these findings and that  $\gamma$  of (001) BFO film is much larger than  $\eta^{\text{max}}$ , Eq. (5) indicates an substantial priority of 71° ferroelastic switching and still implies possible coexistence of 109°- and 180°-switched polarizations, which has been observed in (001) BFO film.<sup>12,13</sup> Moreover, our prediction that 71° ferroelastic switching required lower energy compared with the other two types, shows complete agreement with currently proposed relaxation-mediated ferroelectric switching.<sup>11</sup> However, when it comes to (110)-oriented BFO film, a clear difference lies in the orientation change in dielectric anisotropy from the above (001) to lattice-in-plane diagonal direction [Fig. 1(b)]. This deviation makes  $\gamma > 1$  hold within domain nucleation in (110) BFO film and further  $2\eta^2 < \gamma^2 < 3\eta^2$  tenable to predicate a sequence of 180° → 109° → 71° polarization switching, which consists nicely with available experiments.<sup>8</sup>

As far as the multiphase competition in (001) BFO film is concerned, the minimal tip-bias is governed by the voltage-dependent decrease in  $n$  and  $\eta$ . Although both parameters monotonously influence the critical radius, the dependence of  $Q_\varphi$  on  $\eta$  is found to be dominated by both the switching mode and temporal value of  $n$ . To reduce the complexity of Eq. (5), it is important to note that  $\zeta$  has negligible effects on the curve shape of  $\eta$ -dependent  $Q_\varphi$ , even though it dominates the  $Q_\varphi$  magnitude. Hence,  $\zeta$  can be simplified by a small number with the generality of the findings maintained. First, search for the upper-bound of the varying  $n$  in a (001) BFO film, based on the reported 71° ferroelastic switching temporally followed by ferroelectric domain breakdown (FDB) (Ref. 23) and a sudden decrease in minimal nucleation field.<sup>26</sup> These observations indicate the existence of peaks on the  $Q_\varphi(\eta, n)$  surface for  $0 < \eta \leq \eta^{\text{max}}$ . Thus, we can infer from Fig. 2(a) that the anisotropy exponent of 71° switching  $n_{71^\circ}$  is in the range of (1.5, 1.78). Furthermore,  $\partial Q_\varphi / \partial n < 0$  implies that the variation in  $n$  for 109° or 180° switching is in the range of  $[1, n_{71^\circ}]$ . Note that the exponent,  $2/(2n+1)$ , of the minimum charge (or the coercive tip-bias) obtained and the variation in  $n$  in the range of  $[1, n_{71^\circ}]$  for the



ferroelectric polarization switching in MFs BFO film, are highly expected to be closely related to the fractal dimensionality of ferroelectric DW, such as the Pb(Zr,Ti)O<sub>3</sub> DWs measured by Jo *et al.*<sup>27</sup> and Paruch *et al.*<sup>28</sup> recently.

Compared with the nonlinear evolution of minimal energy for the 71° switching, either the 109° or 180° switching is associated with a monotonic but more rapid increase in the required tip-bias. In other words, the condition of  $\partial Q_\varphi / \partial \eta < 0$  is strictly adhered to the 109°/180°-switched domain growth (not shown here). Since applying a finite tip-bias can only switch a limited ( $\eta \neq 0$ ) domain volume, it is reasonable to identify both the 109° and 180° switching with an activation mode.<sup>22</sup> On the contrary, the 71°-switched domains can penetrate through the whole thickness of (001) BFO film ( $\eta=0$ ),<sup>13</sup> as long as the applied voltage exceeds a critical value,<sup>19,29</sup> called FDB bias, which is labeled as a solid diamond in Fig. 2(a).

Validation of Eq. (5) by the existing results will be performed below. By adopting an approach consistent with the measured coercive bias of BFO film<sup>22</sup> and experimental procedures,<sup>13,26</sup> the ratio of  $M_{71^\circ}/M_{180^\circ}$  [ $M$  is as defined in Eq. (2)] is determined to be  $\sim 15$ , which is much larger than  $M_{109^\circ}/M_{180^\circ}$  of  $\sim 1.75$  when  $\zeta=0.1$  is used. Equation (2) shows that, apart from high heterogeneity level, the dramatic energy-lowering of 71° ferroelastic switching can also be attributed to its highly sensitive adaptation of DW width to domain shape elongation. Our theoretical results of the competitive multipolarization switching in (001) epitaxial BFO film are displayed in Fig. 2(b). It can be seen that a lower tip-voltage (about 3.5 V) induces 71° polarization switching by overcoming the intrinsic energy barrier between the switched  $\mathbf{P}_{71^\circ}$  and initial  $\mathbf{P}_0$  state; on increasing the tip-bias, domains with  $\mathbf{P}_{109^\circ}$  and  $\mathbf{P}_{180^\circ}$  states start to nucleate at about 4.75 V (point A) and 5 V (point B), respectively. However, a much larger voltage (5.35 V) will activate the occurrence of 71°-switched domain FDB, and simultaneously drive the already nucleated 109° and 180°-switched domains to grow larger along the  $\eta$ -decreasing direction until their equilibrium sizes are approached at the largest tip-bias. It is estimated that the equilibrium radii of 109° and 180°-switched domains stop to grow when  $\eta$  reaches its lower bound of  $\eta_{109^\circ}^{\min} \approx 0.135$  and  $\eta_{180^\circ}^{\min} \approx 0.144$  at 6.5 V. The BFO switching predictions based on Eq. (5) are in excellent agreement with the phase-field results<sup>13</sup> as shown in Figs. 3(a) and 3(b), which demonstrated that 71°-switched domains nucleated at 3.55 V and then spanned the film thickness at 4.55–6.55 V, and that 180° switching started at about 4.55 V. In view of the minor deviations between their minimal biases, our proposed mechanism predicts a high probability that the 109° and 180° switching would coexist in an actual tip poling process, as observed experimentally.<sup>11,13</sup> Besides, it is crucial to note that both charged defects<sup>7</sup> and compressive strains imposed by the substrate<sup>8,10</sup> are also found to significantly affect the intrinsic energy barrier. As for the lack of reports on experimentally observed FDB in (001) BFO films, it may be mainly due to the lack of three-dimensional characterization of the as-poled domain patterns. Besides, it is worth noting that our theoretical prediction and the phase-field-validated FDB phenomenon of 71°-switched domains is not

out-of expectation because BFO has the same symmetry as that of LiNbO<sub>3</sub>, which possesses the most favorable properties for FDB.<sup>19,29</sup> The variation in DW width with an increasing tip-bias can also be obtained from Eq. (5), which indicates a continuous broadening of the wall thickness with an increasing tip field. This is in agreement with the recent phase-field solution, which showed an increase in charged DW width during domain vertical growth.<sup>22</sup> In short, the excellent agreement between our analytical predictions and the existing experimental data<sup>8,11,13</sup> and phase-field results<sup>13,22</sup> demonstrates that our proposed mechanism, which includes the switching inhomogeneity and evolution of DW width, is capable of explaining the competitive multipolarization switching of high complexity in epitaxial BFO films.

Inspired by the distinct transition modes between the FDB mode of 71° polarization switching and the activation mode of 180°/109° switching, we would now propose a brand-new procedure to fabricate single-phase 71° ferroelastic domains in (001) BFO films. Note that the FDB bias curve in Fig. 2(b) actually acts as the envelope and upper-bound of the minimal tip-bias of 71° switching, below which FDB of 71°-switched domain can occur with a series of final domain shape, e.g.,  $\eta=0.06$  or  $10^{-3}$ , as shown in Fig. 2(b). Hence, by applying tip-voltages (e.g., 5.35 V–6.5 V) larger than 71° FDB bias, as shown in Fig. 3(c), 71°-switched domains will grow through the whole sample thickness, whereas the coexisted 180°/109°-switched domains can only grow in a thinner film layer. Second, certain methods such as electrochemical polishing, focused ion beam, etc., can be used to thoroughly remove the thin upper layer so that the undesired domains with mixed polarization states are eliminated. Finally, the remaining film will consist only 71°-switched domains. Moreover, by employing a tip-array<sup>30</sup> coupled with time-dependent tip-bias, we could obtain a 71° ferroelastic domain array of controllable density, which may have wide applications in MF and/or DW devices.

Finally, the following issues are worth addressing in future research: (1) to fully understand the complicated polarization switching in MFs, it is fundamental to experimentally investigate the  $n$  dependence of  $\eta$ , and the  $\varphi$ -dependent sensitivity of DW width evolution and the related variation in DW energy, which has been reported to be factors that dominate the thermodynamic stability of switched domains;<sup>8,11</sup> (2) although the single-phase FDB always require high-voltage SPM,<sup>19,29,30</sup> functionalizing the SPM-tips with conductive nanotubes<sup>31,32</sup> is expected to greatly decrease the minimal FDB bias and thus making it feasible to experiment FDB in (001)-oriented BFO film; (3) since the distinct switching modes in BFO films come from different ranges of  $n$  variation and external field direction, it is of practical importance to either applying a more complex time-dependent tip-bias instead of a constant one to optimally acquire the most desired switching path, or to control temporal variation in  $n$  by chemical doping or tuning the concentration of mobile charged defects; (4) the inclusion of an anisotropy exponent  $n$  in the EK's law has been demonstrated to be very effective in lowering the dynamics of domain nucleation. Thus, it could possibly pave a pathway for better explanation of the

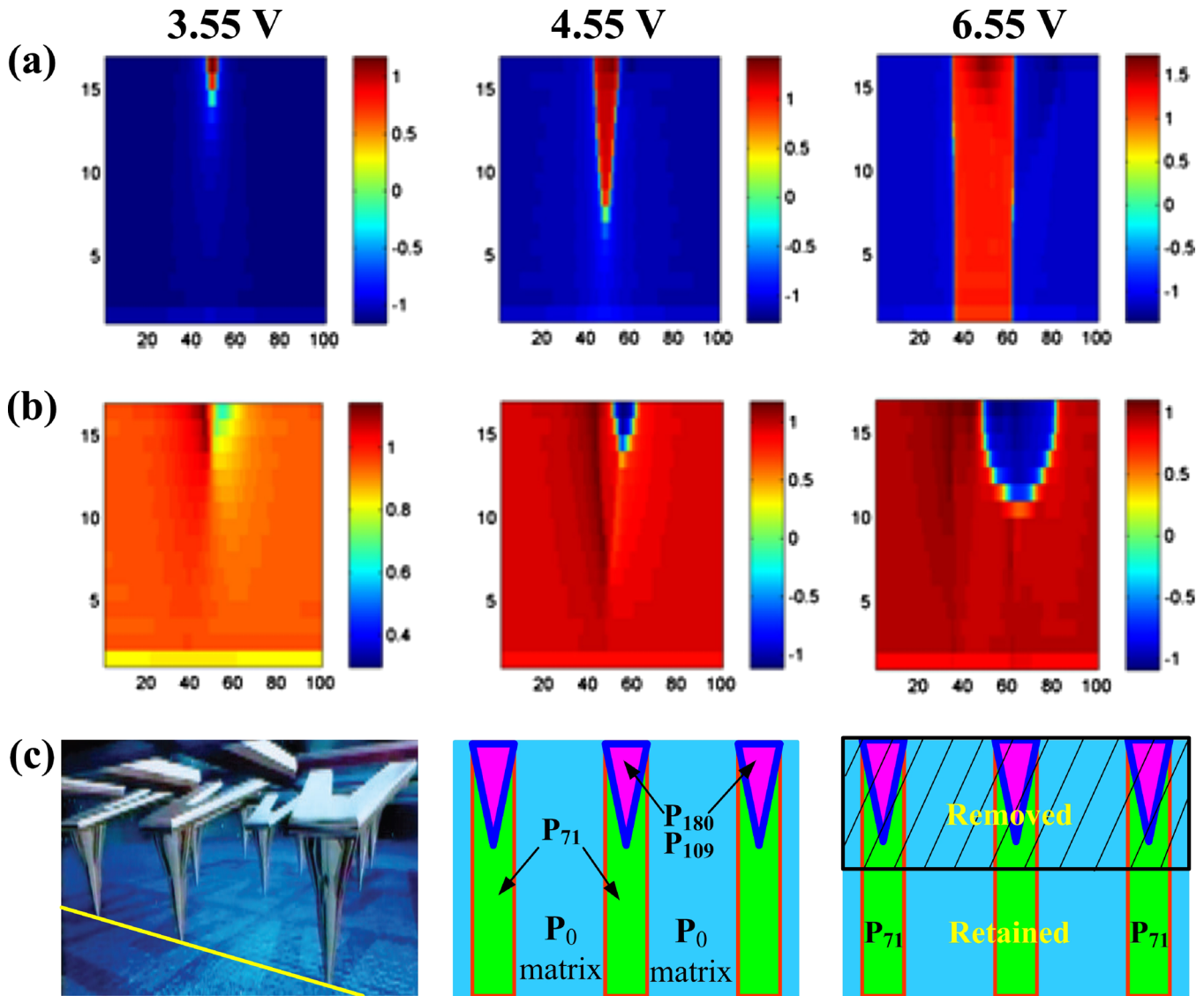


FIG. 3. (Color online) Phase-field simulation results of Ref. 13 for multipolarization evolutions in (001)-oriented BFO film, activated by a series of SPM-tip biases, for case (a)  $71^\circ$  ferroelastic switching and (b)  $180^\circ$  ferroelectric switching, (c) proposed two-step procedure for fabrication of single-phase  $71^\circ$  ferroelastic domain array of controllable density in (001) epitaxial BFO film. The center and right figure of (c) are the cross-sectional schematics of tip-array-poled domain structure and polarization states along the yellow line shown in the first figure of (c) extracted from Ref. 32.

current discrepancy between theoretical prediction and experimental observation in the coercive field,<sup>9</sup> as well as the distinct DW-type-dependent contributions on ME coupling,<sup>1,23,24</sup> photovoltage,<sup>2</sup> and conduction property.<sup>3</sup>

#### IV. CONCLUSION

In summary, the complicated multipolarization switching in both (001) and (110) epitaxial BFO films has been studied using the proposed anisotropic mechanism. By introducing an anisotropy exponent to describe the intrinsic switching inhomogeneity, the fundamental evolution of DW width throughout the biased-tip poling process has been studied, to our knowledge, for the first time by coupling the EK law. It has been found that distinct switching modes, i.e., the FDB mode of  $71^\circ$ -switched domain and the activation mode of  $180^\circ/109^\circ$  switching, exist and dominate the switching forms in the whole domain switching process. These distinct modes can be attributed to different level of inhomogeneity and di-

verse sensitivity of DW width evolution. Our predicted transition orders of  $71^\circ \rightarrow 109^\circ/180^\circ$  switching in (001) BFO film and  $180^\circ \rightarrow 109^\circ \rightarrow 71^\circ$  switching in (110) film are in good agreement with the existing experimental data and phase-field simulation results. In addition, a two-step procedure of substantial technological importance has also been proposed to fabricate single-phase  $71^\circ$  ferroelastic domain array of controllable density in (001) epitaxial BFO films. Finally, possible research topics have been pointed out for future study.

#### ACKNOWLEDGMENTS

Support from the Research Grants Council of the Hong Kong Special Administrative Region (Project Nos. HKU716007E and 716508E) is acknowledged. G.J.W. acknowledges the support of NSF Grant No. CMS 0510409 and the University of Hong Kong Visiting Research Professor Scheme.

## APPENDIX: MODIFICATION OF KITTEL'S LAW

The modification of the original Kittel law to obtain Eq. (2) is illustrated as follow. Based on the existing theoretical works<sup>33-37</sup> on minimization of free energy in free-standing thin films of switchable materials, the standard Kittel law can be expressed as<sup>18</sup>

$$w^2 = C \times \delta \times d, \quad (\text{A1})$$

where  $w$ ,  $\delta$ , and  $d$  denote the periodicity of equilibrium domain size, DW width and film thickness, respectively, and  $C$  is defined as a dimensionless constant independent of the above parameters. Note that Eq. (A1) is only applicable in the case of free-standing film at equilibrium polarization state. However, in order to describe the complicated dynamic domain evolution in a MF BFO film induced by a SPM-tip activated electric field, by replacing  $w$  and  $d$  by the in-plane domain radius  $r$  and the reverted domain length  $l$ , respectively, and noting that the domain aspect ratio  $\eta = \gamma r/l$ , Eq. (A1) can be expressed as

$$r \times \eta = \gamma \times C \times \delta. \quad (\text{A2})$$

Furthermore, by defining  $M = \gamma \times C$  and introducing an anisotropy exponent for the dynamic domain size to include the inhomogeneous nature of SPM-tip activated polarization switching; the EK law can thus be extended to study anisotropic case, as given by Eq. (2).

- <sup>1</sup>W. Eerenstein, N. D. Mathur, and J. F. Scott, *Nature (London)* **442**, 759 (2006).  
<sup>2</sup>S. Y. Yang, J. Seidel, S. J. Byrnes, P. Shafer, C.-H. Yang, M. D. Russell, P. Yu, Y.-H. Chu, J. F. Scott, J. W. Ager, L. W. Martin, and R. Ramesh, *Nat. Nanotechnol.* **5**, 143 (2010).  
<sup>3</sup>J. Seidel, L. M. Martin, Q. He, Q. Zhan, Y.-H. Chu, A. Rother, M. E. Hawkrige, P. Maksymovych, P. Yu, M. Gajek, N. Balke, S. V. Kalinin, S. Gemming, F. Wang, G. Catalan, J. F. Scott, N. A. Spaldin, J. Orenstein, and R. Ramesh, *Nature Mater.* **8**, 229 (2009).  
<sup>4</sup>T. Choi, Y. Horibe, H. T. Yi, W. Wu, and S.-W. Cheong, *Nature Mater.* **9**, 423 (2010).  
<sup>5</sup>L. Hong, A. K. Soh, Q. G. Du, and J. Y. Li, *Phys. Rev. B* **77**, 094104 (2008).  
<sup>6</sup>D. Shilo, H. Drezner, and A. Dorogoy, *Phys. Rev. Lett.* **100**, 035505 (2008).  
<sup>7</sup>S. Jesse, B. J. Rodriguez, S. Choudhury, A. P. Baddorf, I. Vrejoiu, D. Hesse, M. Alexe, E. A. Eliseev, A. N. Morozovska, J. Zhang, L.-Q. Chen, and S. V. Kalinin, *Nature Mater.* **7**, 209 (2008).  
<sup>8</sup>M. P. Cruz, Y. H. Chu, J. X. Zhang, P. L. Yang, F. Zavaliche, Q. He, P. Shafer, L. Q. Chen, and R. Ramesh, *Phys. Rev. Lett.* **99**, 217601 (2007).  
<sup>9</sup>S. Choudhury, Y. L. Li, N. Odagawa, A. Vasudevarao, L. Tian, P. Capek, V. Dierolf, A. N. Morozovska, E. A. Eliseev, S. Kalinin, Y. Cho, L.-Q. Chen, and V. Gopalan, *J. Appl. Phys.* **104**, 084107 (2008).  
<sup>10</sup>G. Catalan and J. F. Scott, *Adv. Mater. (Weinheim, Ger.)* **21**, 2463 (2009).  
<sup>11</sup>S. H. Baek, H. W. Jang, C. M. Folkman, Y. L. Li, B. Winchester, J. X.

- Zhang, Q. He, Y. H. Chu, C. T. Nelson, M. S. Rzechowski, X. Q. Pan, R. Ramesh, L. Q. Chen, and C. B. Eom, *Nature Mater.* **9**, 309 (2010).  
<sup>12</sup>B. J. Rodriguez, S. Choudhury, Y. H. Chu, A. Bhattacharyya, S. Jesse, K. Seal, A. P. Baddorf, R. Ramesh, L.-Q. Chen, and S. V. Kalinin, *Adv. Funct. Mater.* **19**, 2053 (2009).  
<sup>13</sup>N. Balke, S. Choudhury, S. Jesse, M. Huijben, Y. H. Chu, A. P. Baddorf, L. Q. Chen, R. Ramesh, and S. V. Kalinin, *Nat. Nanotechnol.* **4**, 868 (2009).  
<sup>14</sup>G. J. Weng and D. T. Wong, *J. Mech. Phys. Solids* **57**, 571 (2009).  
<sup>15</sup>B. Dupé, I. C. Infante, G. Geneste, P.-E. Janolin, M. Bibes, A. Barthélémy, S. Lisenkov, L. Bellaiche, S. Ravy, and B. Dkhil, *Phys. Rev. B* **81**, 144128 (2010).  
<sup>16</sup>F. Falk, *Z. Phys. B* **51**, 177 (1983).  
<sup>17</sup>Y. Xiao, V. B. Shenoy, and K. Bhattacharya, *Phys. Rev. Lett.* **95**, 247603 (2005).  
<sup>18</sup>A. Schilling, T. B. Adams, R. M. Bowman, J. M. Gregg, G. Catalan, and J. F. Scott, *Phys. Rev. B* **74**, 024115 (2006).  
<sup>19</sup>Y. P. Shi, L. Hong, and A. K. Soh, *J. Appl. Phys.* **107**, 124114 (2010).  
<sup>20</sup>Refer to the (001) epitaxial BFO film shown in Fig. 1(a), it is a known fact that SPM measurements of DW width are always taken on the upper surface of film sample, i.e. the upper (001) plane of the BFO lattice. For the 109° and 180° polarization switching processes, the geometric factor should be identical to the length ratio between each spatial PDV and the corresponding in-plane line projection. Therefore,  $C = \sqrt{2}$  and  $\sqrt{3}/\sqrt{2}$  for 109° and 180° switching, respectively; whereas, for the case of 71° switching in the (001) film, since the in-plane projection of  $\Delta P_{71^\circ}$  is zero, the geometry calculation yields  $H/\delta = l/r = \gamma/\eta$ . Similarly, the geometric factors of the (110) BFO film are determined as  $\sqrt{2}$ ,  $\gamma/\eta$ , and  $\sqrt{3}$  for the 71°, 109°, and 180° switching, respectively.  
<sup>21</sup>Y. C. Chen, Q. R. Lin, and Y. H. Chu, *Appl. Phys. Lett.* **94**, 122908 (2009).  
<sup>22</sup>A. N. Morozovska, E. A. Eliseev, Y. Li, S. V. Svechnikov, P. Maksymovych, V. Y. Shur, V. Gopalan, L. Q. Chen, and S. V. Kalinin, *Phys. Rev. B* **80**, 214110 (2009).  
<sup>23</sup>M. Daraktchiev, G. Catalan, and J. F. Scott, *Phys. Rev. B* **81**, 224118 (2010).  
<sup>24</sup>K. L. Livesey, *Phys. Rev. B* **82**, 064408 (2010).  
<sup>25</sup>A. Lubk, S. Gemming, and N. A. Spaldin, *Phys. Rev. B* **80**, 104110 (2009).  
<sup>26</sup>S. V. Kalinin, B. J. Rodriguez, S. Jesse, Y. H. Chu, T. Zhao, R. Ramesh, S. Choudhury, L. Q. Chen, E. A. Eliseev, and A. N. Morozovsk, *Proc. Natl. Acad. Sci. U.S.A.* **104**, 20204 (2007).  
<sup>27</sup>J. Y. Jo, S. M. Yang, T. H. Kim, H. N. Lee, J.-G. Yoon, S. Park, Y. Jo, M. H. Jung, and T. W. Noh, *Phys. Rev. Lett.* **102**, 045701 (2009).  
<sup>28</sup>P. Paruch, T. Giamarchi, and J.-M. Triscone, *Phys. Rev. Lett.* **94**, 197601 (2005).  
<sup>29</sup>M. Molotskii, A. Agronin, P. Urenski, M. Shvbelman, G. Rosenman, and Y. Rosenwaks, *Phys. Rev. Lett.* **90**, 107601 (2003).  
<sup>30</sup>Y. Rosenwaks, D. Dahan, M. Molotskii, and G. Rosenman, *Appl. Phys. Lett.* **86**, 012909 (2005).  
<sup>31</sup>P. Paruch, A.-B. Posadas, M. Dawber, C. H. Ahn, and P. L. McEuen, *Appl. Phys. Lett.* **93**, 132901 (2008).  
<sup>32</sup>P. Zubko and J.-M. Triscone, *Nature (London)* **460**, 45 (2009).  
<sup>33</sup>C. Kittel, *Phys. Rev.* **70**, 965 (1946).  
<sup>34</sup>C. Kittel, *Rev. Mod. Phys.* **21**, 541 (1949).  
<sup>35</sup>T. Mitsui and J. Furuichi, *Phys. Rev.* **90**, 193 (1953).  
<sup>36</sup>V. A. Zhirnov, *Sov. Phys. JETP* **35**, 822 (1959).  
<sup>37</sup>A. L. Roitburd, *Phys. Status Solidi A* **37**, 329 (1976).